Politecnico di Milano

Spacecraft Attitude Dynamics

Academic Year 2023/2024

Project group n.27

Project n.378

Team Members

Person code	Surname	Name	Bachelor (type and University)
10727361	Lakrad	Adam	Aerospace Engineering at Politecnico di Milano
11009775	Vurro	Martina Angela	Aerospace Engineering at Politecnico di Torino
10736840	Ignesti	Samuele	Aerospace Engineering at Politecnico di Milano
10695552	Gualdana	Guglielmo	Aerospace Engineering at Politecnico di Milano

Project specifications

	Assigned specification	**Modifications**	**Motivation modifications**
Platform	Cubesat 12U		
Attitude Parameters	Euler Angles		
Mandatory sensor	Sun Sensor	Magnetometers	Second measurement to realize the algebraic attitude determination, onboard measure of the magnetic field useful for Magnetic Coils
Actuators	3 Magnetic Coils, 1 Inertia Wheel	1 Reaction Wheel	Enhance spacecraft control

Contents

1 Notation

SYMBOL	MEANING
I	Inertia Matrix
a	semi-major axis
e	eccentricity
i	inclination
Ω	RAAN
ω	pericenter anomaly
θ_{orbit}	true anomaly
A	Direction Cosine Matrix
b	body frame
L	Local Vertical Local Horizontal frame
N	Inertial frame
$\underline{\omega}$	angular velocity
n	mean angular velocity
T	revolution period
p	semilatus rectum
R_e	Earth's radius
$\underline{a}$	acceleration
$\underline{r}$	position
R_i	rotation matrix around i-axis
$\underline{M}$	Torque
$\underline{h}$	angular momentum

SYMBOL	MEANING
$\phi\ \theta\ \psi$	Euler Angles
G	constant of universal gravitation
m	mass
P	pressure
F_e	Power
c	speed of light in the vacuum
S_i	sun-spacecraft versor
Ni	normal direction of i-th surface
ρ_s	reflectivity coefficient
ρ_d	diffusion coefficient
A_i	i-th surface
$\underline{B}$	Earth's magnetic field
A_e	attitude error through DCM
$\underline{\alpha}$	small angles b/LVLH
μ	magnetic permeability of the core
$\underline{i}$	current

Table 1: notation table

2 Introduction

The objective of this project is to simulate the complete attitude dynamics of a 12U spacecraft that performs a Low Earth Orbit.
In order to guarantee specific pointing performances, an active control loop has been implemented.
First of all, the spacecraft geometry has been defined, as shown in figure 1

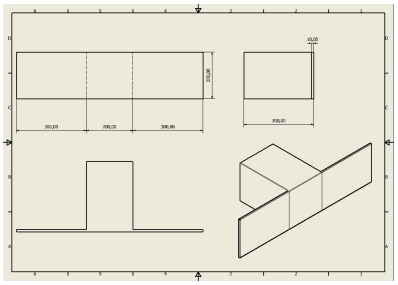

Figure 1: 12U cubesat CAD

	Mass $[kg]$	Size $[m]$
Main body	14.5091	0.200x0.200x0.300
Single solar panel	0.3628	0.010x0.200x0.300

Table 2: 12U features

From data in Table 2, the principal inertia matrix I has been computed.

$$I = \begin{bmatrix} 0.2453 & 0 & 0 \\ 0 & 0.1872 & 0 \\ 0 & 0 & 0.1644 \end{bmatrix} [kgm^2] \tag{1}$$

Moreover the orbit chosen has the initial parameters reported in Table3.

$a[km]$	e	$i[deg]$	$\Omega[deg]$	$\omega[deg]$	$\theta_0[deg]$
8054.6	0.0100	1.7965	0	1.5708	0

Table 3: Orbital parameters

3 Mission requirements

In this project the analysis of the mission has been done following some given constraints.

- Platform: Cubesat 12U
- Attitude Parameters: Euler Angles
- Mandatory Sensor: Sun Sensor
- Actuators: 3 Magnetic Coils, 1 Inertia Wheel

As reported in the cover, there had been made some modifications to achieve a correct attitude determination and control.
The target requirement of this Nadir pointing mission:

- $A_{b/L} = I_3$
- $\underline{w} = [0\ 0\ n]^T$

where $n = 2\pi/T$

4 Spacecraft dynamics and kinematics

4.1 Orbital Mechanics

The Cubesat follows a LEO Sun-synchronous orbit around the Earth , in order to satisfy the given constraints. The initial orbital parameters, except the inclination, have been chosen to match the usual values for LEO missions, involving Nadir pointing.
A Sun-synchronous orbit, useful when dealing with Sun sensors, is achieved when the precession rate of the spacecraft equals the mean motion of the Earth around the Sun, obtaining:

$$\cos i = \frac{-2\rho a^{\frac{7}{2}}}{3J_2 R_e^2 \mu} \tag{2}$$

To compute the position and velocity vector during the orbital period, it has been integrated the restricted two body problem, taking into account the presence of the J_2 effect, due to Earth's oblateness

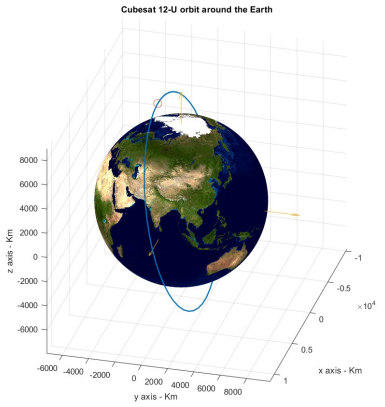

$$\frac{d\underline{r}^2}{dt^2} = -\mu\frac{\underline{r}}{||r||^3} + \underline{a}J_2 \tag{3}$$

Figure 2: Cubesat orbit around the Earth

There have also been computed the keplerian elements from position and velocity vectors,to define A_{goal}, which for Nadir pointing is simply the matrix from local vertical local horizontal (LVLH) reference frame to inertial reference frame:

$$A_{L/N} = R_3(\omega + \theta)R_1(i)R_3(\Omega) \tag{4}$$

It has been solved the restricted two body problem (neglecting perturbations) between Earth and Sun in a SCI(Sun Centred Inertial) reference frame and rotated the spacecraft-earth position vector from ECI(Earth Centred Inertial) to SCI, in order to obtain the spacecraft position at each time step in SCI, useful for further analysis as shown in Chapters 5.2 and 6.1.1

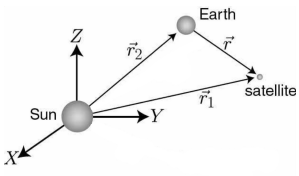

Figure 3: spacecraft , Earth , Sun system in SCI

All of these parameters are computed in the Simulink block "Orbit Dynamics"

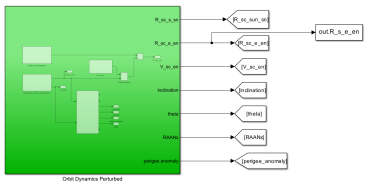

Figure 4: ORBIT DYNAMICS

4.2 Dynamics: Euler equation

The dynamics of the Cubesat has been computed through the Euler Equations, assuming that the spacecraft is rigid and with the body fixed frame that coincide with the principal axis frame:

$$I\dot{\underline{\omega}} = I\underline{\omega} \times \underline{\omega} + \underline{M}_{act} + \underline{M}_{dist} \tag{5}$$

As it will be shown in chapter 8.2, the Cubesat is equipped with an Inertial Wheel, mounted along the spacecraft's pitch axis, which is able to provide a passive stabilization, thanks to its constant relative spin rate, alongside with the opportunity provide active control, by tuning it's

angular acceleration. The inertia wheel contribute $\underline{\omega} \wedge A\underline{h}_r + A\dot{\underline{h}}_r$ has been directly considered in $\underline{M}_{act}$ in Eq. 5.
In torque free motion hypothesis, with a proper ω_r it's possible to enlarge the stability region, making ,into certain conditions, also the intermediate and minimum Inertia axis stable. In the studied case, it has been chosen to mount the Inertia Wheel with its axis aligned with the minimum inertia axis (z axis, in body frame). Using non-dimensional coefficients $K_{roll}\, K_{yaw}\, K_{pitch}$,it's possible to visualize the stability diagram:

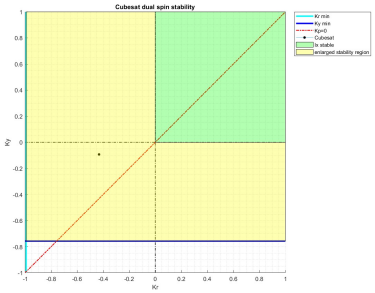

Figure 5: stability diagram with $\underline{\omega}_r = [0\ 0\ 0.85]^T\, rad/s$

The stable condition can be observed also in the state phase planes:

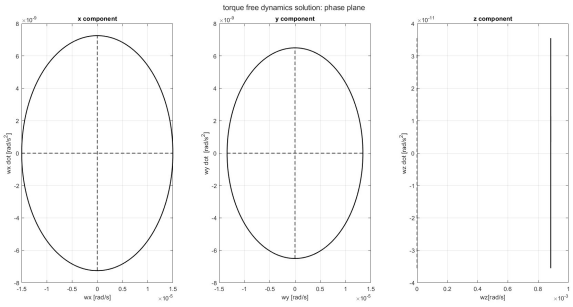

Figure 6: phase plane

To obtain Figure 6 it has been used a perturbed
$\underline{\omega}_0 = [1e-5\ ,1e-5\ ,n+1e-5]^T\, rad/s$, $A_0 = A_{goal,t=0}$, with a simulation time equal to two revolutions. All of these parameters are computed in the Simulink block "Euler equation"

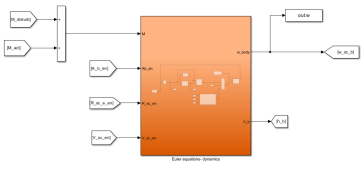

Figure 7: EULER EQUATION

4.3 Kinematics: Euler Angles

As required, the attitude of the Cubesat has been described through Euler Angles, which allow to represent a complete attitude of an orthogonal frame as the multiplication of three trivial and independent rotations.
As a general rule, the rotations described with all different indexes are suitable for small rotations(e.g. 312) whereas, with first and last index equal, for large rotations(e.g. 313). The time derivatives for Euler angles, for 312 configurations, are computed using:

$$\begin{cases} \dot{\phi} = \dfrac{\omega_z cos(\psi) - \omega_x sin(\psi)}{cos(\theta)} \\ \dot{\theta} = \omega_x cos(\psi) + \omega_z sin(\psi) \\ \dot{\psi} = \omega_y - [\omega_z cos(\psi) - \omega_x sin(\psi)] \dfrac{sin(\theta)}{cos(\theta)} \end{cases} \tag{6}$$

It's possible to build the DCM from the Euler angles:

$$A_{312} = \begin{bmatrix} cos\psi cos\phi - sin\psi sin\phi sin\theta & cos\psi sin\phi + sin\psi cos\phi sin\theta & -sin\psi cos\theta \\ -sin\phi cos\theta & cos\phi cos\theta & sin\theta \\ sin\psi cos\phi + cos\psi sin\phi sin\theta & sin\psi sin\phi - cos\psi cos\phi sin\theta & cos\psi cos\theta \end{bmatrix} \tag{7}$$

For most of its lifetime, the Cubesat will operate small rotations, therefore the 312 configuration it's the preferred one. However, this configuration has a singularity for $\theta = \dfrac{\pi}{2} + k\pi$. To solve this, it was necessary to compute also the kinematics for 313 configuration, which has a singularity for $\theta = k\pi$; lastly a logic was implemented to switch from one configuration to the other whenever it was close enough to the singularity of the adopted sequence .
To validate that the procedure is correct, it was verified the constancy of the vector angular momentum, in torque free motion in an inertial reference frame:

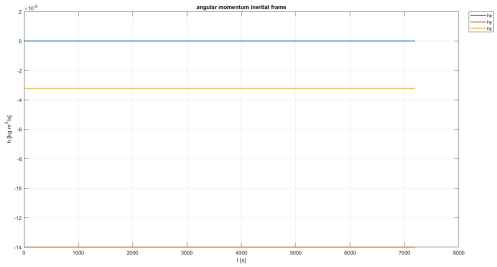

$$\dot{\underline{h}}_N = \underline{M}_N = 0$$
$$\underline{h}_N = A_{b/N}^T \, \underline{h}_b = A_{b/N}^T \, I \, \underline{w}_b$$

Figure 8: h_N

All of these parameters are computed in the Simulink block "Kinematics"

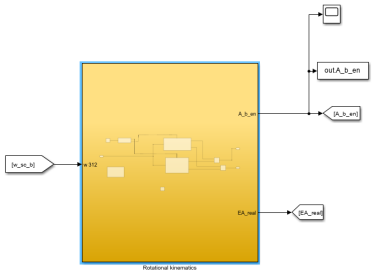

Figure 9: KINEMATICS

5 Environmental disturbances

In this mission the Cubesat is on a low eccentricity LEO orbit. In space applications the main disturbance torques are:

- Gravity Gradient torque
- Magnetic torque
- Solar Radiation Pressure
- Aerodynamic Drag torque

5.1 Gravity gradient

Due to the non uniformity of the gravitational field over the Cubesat, a system of non parallel forces (each aligned with its proper local vertical), generate a non-negligible torque over the satellite. The torque is computed by integrating, over the Cubesat mass, the gravitational torque acting on the elementary mass, with respect to the center of mass. This procedure leads to:

$$\underline{M} = -\frac{3Gm_e}{||\underline{r}||^3} I\underline{c} \times \underline{c} \tag{8}$$

where $\underline{c}$ is:

$$\begin{bmatrix} c_1 \\ c_2 \\ c_3 \end{bmatrix} = \mathbf{A_{b/L}} \begin{bmatrix} 1 \\ 0 \\ 0 \end{bmatrix} \tag{9}$$

It's possible to study the effect of the gravity gradient on the spacecraft's stability, under the hypothesis of circular orbit and linearised dynamics.

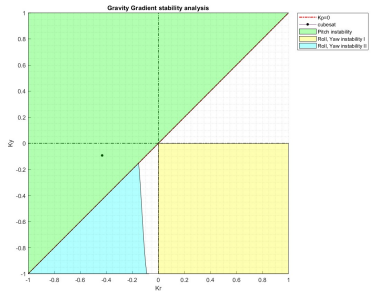

Figure 10: Gravity Gradient effect on stability

The gravity gradient contribute is destabilizing, however with attitude control and dual spin stabilization, this effect will be compensated, also in view of the observation made later in Eq. (19).

5.2 Solar Radiation Pressure

The solar radiation illuminating the outer surface of the Cubesat generates a pressure, therefore a force and a torque around the center of mass of the satellite. The main sources of electromagnetic radiation are:

- direct radiation of the Sun(1358 $\frac{W}{m^2}$ at 1 UA)
- solar radiation reflected by the Earth (29% of the direct sun radiation)
- Earth's own radiation (143.4 $\frac{W}{m^2}$)

The pressure is therefore:

$$P = F_e/c \tag{10}$$

To obtain the torque, the Cubesat is decomposed as a set of flat surfaces, each of which with a proper diffusion and specular reflection coefficients, area and normal versor. Knowing the Sun's direction in body frame $s_{\text{sun}_b} = A_{b,N} s_{\text{sun}_n}$ and the Earth's direction in body frame $s_{\text{earth}_b} = A_{b,N} s_{\text{earth}_n}$:

$$\underline{M}_{SRP} = \begin{cases} \sum_{i=1}^{n_{surface}} \underline{r_i} \times \underline{F_i} \\ 0 \end{cases} \tag{11}$$

where if $\hat{S}_b \cdot \hat{N}_{bi} > 0$:

$$\underline{F_i} = -PA_i(\hat{S}_b \cdot \hat{N}_{bi})[(1-\rho_s)\hat{S}_b + (2\rho_s(\hat{S}_b \cdot \hat{N}_{bi}) + \frac{2}{3}\rho_d)\hat{N}_{bi}] \tag{12}$$

where $P = F_{sun}/c$. The previous inequality takes into account the case where the surface may be in shadow, whereas its opposite surface sees the Sun. An analog procedure is followed to compute the torque due to electromagnetic radiation coming from the Earth(M_{ERP}), where it's taken into account the Earth's versor and $P = \dfrac{F_{earth} + F_{reflected}}{c}$

The total torque is

$$M = M_{SRP} + M_{ERP} \tag{13}$$

5.3 Earth magnetic field

5.3.1 Earth magnetic field model

In LEO orbits the effect of the Earth's magnetic field is so important that the torque generated by the interaction with it it's not negligible, indeed, the Cubesat is equipped with 3 magnetic coils to exploit this phenomena. A precise model of the magnetic field is therefore needed. The magnetic field($\underline{B}$) is modelled, in spherical coordinates, as the gradient of a scalar potential(V) , normally modelled as a series expansion of spherical harmonics:

$$\underline{B} = -\underline{\nabla}V \tag{14}$$

$$V(r,\theta,\phi) = R\sum_{n=1}^{k}(\frac{R}{r})^(n+1)\sum_{m=0}^{n}(g_n^m cos(m\phi) + h_n^m sin(m\phi))P_n^m(cos(\theta)) \tag{15}$$

where :

- R : Earth's equatorial radius
- g_n^m and h_n^m: Gaussian coefficients, available in IGRF 13th Gen. (2020) table up to order 13
- r, θ , ϕ : spherical coordinates for satellite position in the Earth Centred Earth Fixed (ECEF) reference frame
- P_n^m :Schmidt quasi normalized associated Legendre polynomial, in this case, for computational reasons, it has been implemented the normalization due to Gauss, which is based on a recursive method.

using Eq. (14):

$$\begin{cases} B_r = -\dfrac{\partial(V)}{\partial(r)} \\ B_\theta = -\dfrac{1}{r}\dfrac{\partial(V)}{\partial(\theta)} \\ B_\phi = -\dfrac{1}{rsin(\theta)}\dfrac{\partial(V)}{\partial(\phi)} \end{cases} \tag{16}$$

Then to express the Magnetic field in body frame, it has to be firstly transformed in inertial frame using the declination $\delta(t)$ and the right ascension $\alpha(t)$. Then, $B_b = A_{b/N}B_n$.

5.3.2 Magnetic torque computation

Once computed the magnetic field model in body frame, depending only on time, it's possible to compute the Magnetic field disturbance.

$$\underline{M}_{magn} = \underline{m} \times \underline{B}_b \tag{17}$$

where $\underline{m}$ is the internal residual dipole, caused by circulating current in wires and electronics. To have an estimation, the worst case scenario is considered, where: $\underline{m} = [0.1\ \ 0.1\ \ 0.1]' Am^2$

5.4 Drag

The interaction between satellite and Earth's atmosphere generates a set of aerodynamic forces acting on the satellite itself, resulting in a torque , with respect to the center of mass of the satellite. The model adopted to study this disturb is based on the assumption that the air particles hit the external surface of the satellite and their kinetic energy is totally transferred to the satellite. The Cubesat is decomposed as a set of flat surfaces, so that the total torque is computed as the superposition of all the torques.

$$\underline{M}_{drag} = \begin{cases} \sum_{i=1}^{n} \underline{r}_i \times \underline{F}_i \\ 0 \end{cases} \tag{18}$$

If $\hat{N_{b,i}} \cdot \frac{\underline{v}_{rel\ i,b}}{||\underline{v}_{rel\ i,b}||} > 0$: $\quad \underline{F}_i = -\frac{1}{2}\rho c_d v_{rel,i\ b}^2 \frac{\underline{v}_{rel\ i,b}}{||\underline{v}_{rel\ i,b}||}(\hat{N_{b,i}} \cdot \frac{\underline{v}_{rel\ i,b}}{||\underline{v}_{rel\ i,b}||})A_i$

- ρ : air density modelled by interpolating the data set provided during lecture, until 1000 km. Above the density is supposed to be constant
- c_d: drag coefficient depending on the angle of attack and roughness of the surfaces. $c_d \approx 3$
- $\underline{v}_{rel\ i,b}$: relative velocity between the i-th panel and the Earth's atmosphere, assumed to rotate with the Earth.
- $\underline{r}_i = \underline{r}_{cp,i} - \underline{r}_{cg}$

5.5 Disturbances Comparison

To determine the two most significant disturbances, it has been made a preliminary estimation of the relevance of the torques, considering for each disturb the worst case scenario:

- Gravity Gradient: $T_{max} = \frac{3Gm_t}{2r^3}|I_M - I_m| = 2.7232\,e-7\,Nm$
- Solar Radiation: $T_{max} = P_s A_s(1+q)(r_{ps} - r_{cg}) = 2.8079\,e-8\,Nm$
- Magnetic Field: $T_{max} = D_s B_{max} = 2.7667\,e-6\,Nm$
- Aerodynamics: $T_{max} = \frac{1}{2}\rho v_{rel}^2 A_s c_d(r_{pa} - r_{cg}) = 2.0574\,e-12\,Nm$

The most significant disturb is the magnetic field as the its influence on satellites in LEO orbits is very important; furthermore the least significant disturb is the aerodynamic drag , being mostly significant for satellites orbiting at altitudes lower than 400 Km. The gravity gradient appears to be the second most significant disturb. However, since a Nadir pointing is analysed, this disturb during the pointing phase becomes zero as the body reference frame tends to match the LVLH reference frame, from Eq. 9:

$$\begin{bmatrix} c_1 \\ c_2 \\ c_3 \end{bmatrix} = \mathbf{A_e} \begin{bmatrix} 1 \\ 0 \\ 0 \end{bmatrix} \approx \begin{bmatrix} 1 \\ 0 \\ 0 \end{bmatrix} \tag{19}$$

where $A_e = A_{b/N}\, A_{L/N}^T = A_{b/L}$ is the attitude error and it tends to be an identity matrix during the pointing phase. For this reason both the solar radiation and gravity gradient are considered to be relevant disturbs, as during the pointing phase the solar radiation becomes far more significant than the gravity gradient, which tends to zero.
The choice of most significant disturbs is verified by the analysis of their evolution during real mission simulation:

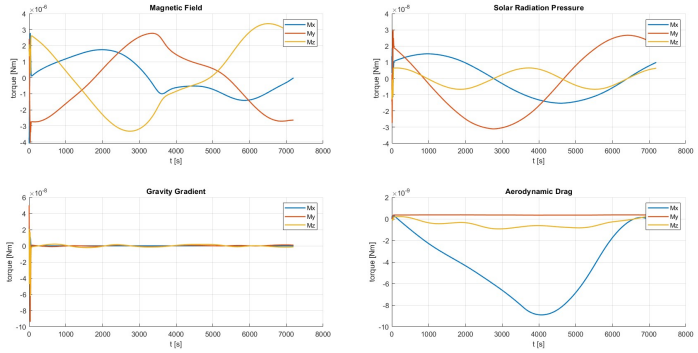

Figure 11: Disturbs over 1 orbit

It's useful to highlight that certain estimated values don't perfectly match with the real trend, as during the estimation it wasn't taken into account coupling effect between the disturbances and the spacecraft attitude and dynamics evolution. The disturbances computation is performed in the Simulink block "Environment Disturbances".

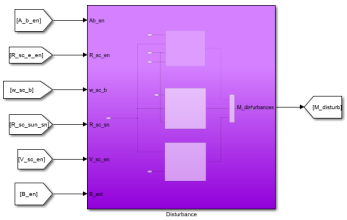

Figure 12: ENVIRONMENT DISTURBANCES

6 Attitude determination system

The sensors are modeled in order to compute the attitude matrix $A_{B/N}$ using an algebraic method. These computations are performed in the Simulink block "Attitude and Error determination".

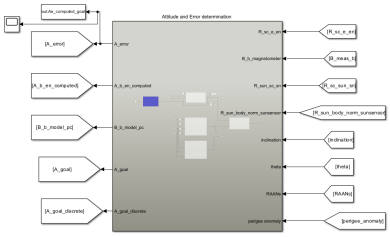

Figure 13: ATTITUDE AND ERROR DETERMINATION

6.1 Sensors

At least two independent measurements are needed to completely determine the orientation of the spacecraft in space. In this specific case of a Sun-Synchronous orbit, the implementation of Sun Sensors and Magnetometers is enough since it can be demonstrated that they provide measurements that are never aligned each other. By using an algebraic method, it is possible to detect the plane containing the two measurements and then the perpendicular direction to this plane. Both sensors are modeled in the Simulink block "Sensors".

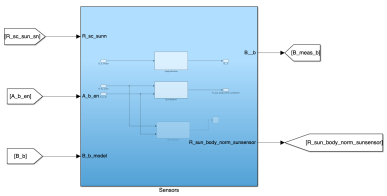

Figure 14: SENSORS

6.1.1 Sun Sensors

Size $[mm]$	Mass $[g]$	FoV $[deg]$	Sampling rate $[s]$	Accuracy $[deg]$	Noise $[deg]$ $RMS/\sqrt{Hz}@1Hz$	Power $[mV]$
24.66x15x3.50	3	110	0.1	< 0.3	$12e{-}12$	$2.5 - 40$

Table 4: Sun Sensors - SS200

The Sun Sensor implemented consists of 6 solar cells placed each on a surface of the Cubesat, in order to guarantee a complete field of view [1]. The measurements of sensors are modeled as the true values obtained from the orbit propagation and spacecraft attitude, superimposed with a random noise whose amplitude is determined by the sensor specifications. Therefore:

$$\underline{s}_b^M = G(s_N) A_{b/N} \underline{s}_N \tag{20}$$

where $\underline{s}_b^M$ is the measured sun-to-spacecraft-distance in body frame, which is affected by errors and distortions $G(\underline{s_N})$ coming from the measurement itself; $\underline{s}_N$ is the Sun-to-spacecraft-distance in inertial frame. Knowing each cell's position, it is possible to compute the angle θ_i between the direction of Sun and the normal vector to the surface at issue $\hat{N}_i$, such that:

$$\hat{N}_i \cdot \underline{s} = cos\theta_i \tag{21}$$

Since there are 6 solar cells with 110° FoV, more than one measurement at the same time can be obtained. In this case, a criterion is chosen in order to minimize the error propagation, that is computing the mean value from the values in body frame. To verify the correct behaviour of the sensors the angle β between the two versors [2] $\underline{r}_{sun\ real}$, $\underline{r}_{sun\ sens}$ was computed.

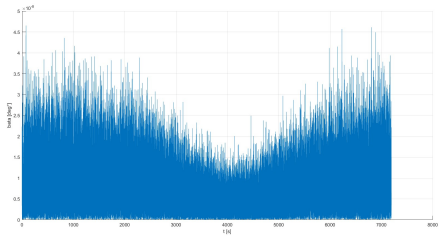

Figure 15: sun sensors error

The value of the angle oscillates around 0 therefore the sun sensors work properly.

[1] The limitation due to the sensors' FoV is taken into account too.
[2] versors in Body frame

6.1.2 Magnetometers

Size $[cm]$	Mass $[g]$	Sampling Rate$[s]$	Accuracy	Sensitivity $[\mu V/nT]$	Noise $RMS/\sqrt{Hz}@1Hz[pT]$	Orthogonality error$[deg]$
3.51x3.23x8.26	100	0.1	$\pm 0.75\%$	100	12	max ± 1

Table 5: Magnetometers MAG-3

A magnetometer consisting in 3 pairs of magnetic cores, each mounted alongside one body axis, provides a vector measurement of the local magnetic field $\underline{B}$. Its implementation is also required to use magnetic coils as actuators, being fundamental an onboard measurement in real time of the magnetic field. Orthogonality errors have to be considered (see Data sheet 5), therefore:

$$\underline{B}_b^M = A_\epsilon A_{b/N} \underline{b}_N \tag{22}$$

$$A_\epsilon = I_3 - [\Theta_\epsilon]^\wedge \tag{23}$$

where B_b^M is the magnetic field measured in body frame; B_N is the magnetic field in inertial frame; $[\Theta_\epsilon]\hat{}$takes into account the errors in axis alignment; I_3 is the identity matrix. To verify the correct behaviour of the magnetometers the angle γ between the two vectors $\underline{B}_{real}$, $\underline{B}_{sens}$ [3] as well as the error in magnitude have been computed.

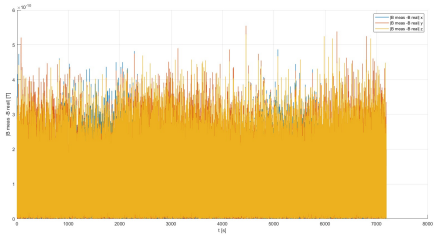

Figure 16: $|\underline{B}_{meas} - \underline{B}_{real}|$

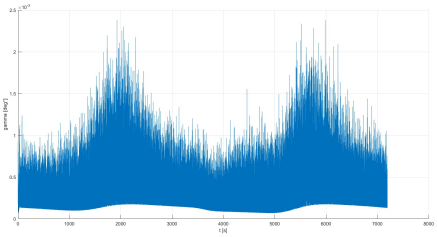

Figure 17: γ

The value of the angle and also of magnitude oscillates around 0 therefore the magnetometers work properly.

6.2 Attitude determination algorithm

Given two independent measurements in body frame $\underline{p}$ and $\underline{q}$ and their corresponding directions in body frame $\underline{a}$ and $\underline{b}$, two orthogonal frames can be associated to the measurements and their reference directions using the following algebraic method:

$$\begin{aligned} \underline{s}_1 &= \underline{p} & \underline{v}_1 &= \underline{a} \\ \underline{s}_2 &= \frac{\underline{p} \times \underline{q}}{|\underline{p} \times \underline{q}|} & \underline{v}_3 &= \frac{\underline{a} \times \underline{b}}{|\underline{a} \times \underline{b}|} \\ \underline{s}_2 &= \underline{p} \times \underline{s}_2 & \underline{v}_3 &= \underline{a} \times \underline{v}_2 \end{aligned} \tag{24}$$

Therefore, the attitude determination algorithm is applied.

$$\begin{aligned} [\underline{s}_1 \ \underline{s}_2 \ \underline{s}_3] &= A_{b/N} [\underline{v}_1 \ \underline{v}_2 \ \underline{v}_3] \\ S &= A_{b/N} V \\ A_{b/N} &= S V^{-1} = S V^T \end{aligned} \tag{25}$$

[3] vectors in Body frame

When computing the attitude, a slightly different B_b model has been used. Since the attitude determination is done by an on-board computer, a lower computational power is available with respect to the one on ground station. This is the reason why a 5th order (instead of a 13th one) magnetic field model has been computed in this Simulink block.
The procedure has been validated through the analysis of the attitude error between the real and the computed attitude, in terms of DCM: $A_e = A^T_{comp\ b/N}\ A_{b/N}$

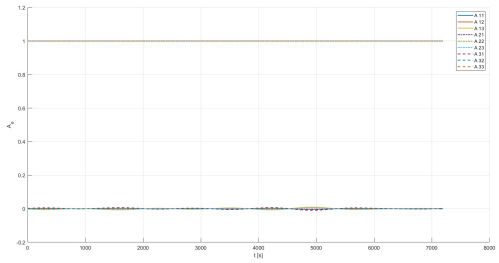

Figure 18: attitude determination error

The small oscillation of the off-diagonal terms is correlated to measurements errors and discretization of the sensors and computer, however, the oscillation is rather small, not affecting significantly the performance.

7 Attitude control system

In this section the control logic and actuators are explained. Two types of control techniques have been used in this project:

- **B-dot Feedback Algorithm**
- **Lyapunov control function**

Both control logic are developed in the Simulink block "Control System" shown below.

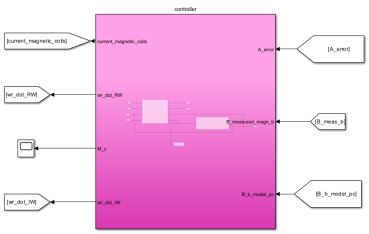

Figure 19: CONTROL SYSTEM

7.1 Control laws

7.1.1 State Space model

In presence of the gravity gradient in the LVLH, taking into account the effect of noise, the real state space of the system is:

$$\begin{cases} \dot{x} = Ax + Bu + Fw \\ y = Cx + Du + v \end{cases} \tag{26}$$

That is, in a more explicit form:

$$\begin{Bmatrix} \ddot{\alpha}_x \\ \ddot{\alpha}_y \\ \ddot{\alpha}_z \\ \dot{\alpha}_x \\ \dot{\alpha}_y \\ \dot{\alpha}_z \end{Bmatrix} = \begin{bmatrix} 0 & (1-K_y)n & 0 & -K_y n^2 & 0 & 0 \\ (K_r-1)n & 0 & 0 & 0 & -4K_r n^2 & 0 \\ 0 & 0 & 0 & -K_y n^2 & 0 & -3K_p n^2 \\ 1 & 0 & 0 & 0 & 0 & 0 \\ 0 & 1 & 0 & 0 & 0 & 0 \\ 0 & 0 & 1 & 0 & 0 & 0 \end{bmatrix} \begin{Bmatrix} \dot{\alpha}_x \\ \dot{\alpha}_y \\ \dot{\alpha}_z \\ \alpha_x \\ \alpha_y \\ \alpha_z \end{Bmatrix} + \begin{bmatrix} \frac{1}{I_x} & 0 & 0 \\ 0 & \frac{1}{I_y} & 0 \\ 0 & 0 & \frac{1}{I_z} \\ 0 & 0 & 0 \\ 0 & 0 & 0 \\ 0 & 0 & 0 \end{bmatrix} \begin{Bmatrix} M_x \\ M_y \\ M_z \end{Bmatrix} + Fw$$

$$y = \begin{Bmatrix} \alpha_x \\ \alpha_y \\ \alpha_z \end{Bmatrix} = \begin{bmatrix} 0 & 0 & 0 & 1 & 0 & 0 \\ 0 & 0 & 0 & 0 & 1 & 0 \\ 0 & 0 & 0 & 0 & 0 & 1 \end{bmatrix} \begin{Bmatrix} \dot{\alpha}_x \\ \dot{\alpha}_y \\ \dot{\alpha}_z \\ \alpha_x \\ \alpha_y \\ \alpha_z \end{Bmatrix} + \begin{bmatrix} 0 & 0 & 0 \\ 0 & 0 & 0 \\ 0 & 0 & 0 \end{bmatrix} \begin{Bmatrix} M_x \\ M_y \\ M_z \end{Bmatrix} + v \tag{27}$$

where w and v are uncorrelated white noise; F is the analogue of B for the disturbances w; K_p, K_r, K_y are respectively the pitch, yaw and roll non-dimensional coefficients.

7.1.2 De-tumbling manoeuvres: B-dot proportional

The B-dot proportional feedback algorithm is used during the De-tumbling phase in which the main objective is to slow down the spacecraft. Three magnetic coils have been used as actuators in order to obtain this control. The control input is

$$\underline{u_c} = \underline{m} \times \underline{B} \tag{28}$$

$$\underline{m} = k_b \dot{B}_m \tag{29}$$

where B_m is the measured magnetic field and k_b is a gain found with a trial and error approach. In order to optimise the De-tumbling phase, different gains for each Torque component have been used.

$$k_b = \begin{bmatrix} 5e7 & 0 & \\ 0 & 7e7 & 0 \\ 0 & 0 & 8e6 \end{bmatrix}$$

If the spacecraft is rotating at a sufficient high angular velocity, then we can assume $\dot{B} \approx 0$. Therefore, it can be assumed that, for sufficiently high ω:

$$\dot{B_m} = -\omega \times B_m \tag{30}$$

When the De-tumbling phase is almost completed and the angular velocity is closer enough to zero,then a slew manoeuvre should be performed in order to point towards the desired target.

7.1.3 Pointing manoeuvre: Lyapunov control functions

In order to do the slew manoeuvre as well as to achieve Nadir pointing - that means to track a time-dependent attitude trajectory (LVLH moving frame) - a non-linear Lyapunov control has been implemented. The objective is to guarantee not only the performance but also the system's asymptotic stability. Therefore, Lyapunov's Second Stability Theorem has been applied.
A suitable Lyapunov cost function based on DCM is:

$$V = \frac{1}{2}\underline{\omega_e}^T I \underline{\omega_e} + 2k_2 tr(I_3 - A_e) \tag{31}$$

That leads to a control input:

$$\underline{u} = -k_1 \underline{\omega_e}^T - k_2 (A_e^T - A_e)^V + \underline{\omega_B} \times I\underline{\omega_B} + I(A_e \underline{\dot{\omega}_d} - [\underline{\omega_e}\wedge] A_e \underline{\dot{\omega}_d}) \tag{32}$$

with

$$A_e = A_{b/N} A_d^T \tag{33}$$
$$\underline{\omega}_e = \underline{\omega}_b - A_e \underline{\omega}_d \tag{34}$$

where A_e is the attitude error; A_d is the goal attitude (desired attitude) that is LVLH moving frame; $\underline{\omega}_d = [0\ 0\ n]'$ is the desired angular velocity and $\underline{\omega}_e$ is the difference between the actual angular velocity in body frame $\underline{\omega}_b$ and the one to be achieved. The gains k_1 and k_2 have been found by using a trial and error method, verifying that they satisfy the condition on the first derivative of the Lyapunov cost function $\dot{V} < 0$, such that the system is asymptotically stable. For slew manoeuvre:

$$k_{1,slew} = 9e-2; \qquad k_{2,slew} = 5e-3$$

For pointing:

$$k_{1,pointing} = 1e-1; \qquad k_{2,pointing} = 0.25e-1$$

Note that for slew and pointing phases the assumption of equal control on three axis has been made.

7.1.4 State Observer

Since no Gyro sensors have been implemented, a state observer is necessary to have a good evaluation of the system's state and, therefore, of the angular velocity of the spacecraft. By using an observer, it is possible to deduce the system's state x by processing the outputs of the real system y given by the sensors. In this project an Optimal Observer (Kalman Observer) has been implemented. Because of the presence of noise that affect the outputs and the estimated attitude, the Kalman Observer is used to filter the signals too. The state observer can be written as:

$$\begin{cases} \dot{\hat{x}} = \hat{A}\hat{x} + \hat{B}u + Ly \\ \hat{y} = \hat{x} \end{cases} \tag{35}$$

The observation error $e = \hat{x} - x$ must be zero once the transient is exhausted. The gain L is computed in such a way that the variance of e is minimised.

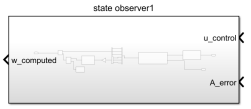

Figure 20: STATE OBSERVER

Once the state has been computed, it is possible to evaluate $\underline{\omega}_B$. For small rotations, angles and eccentricity, the following linearization about the LVLH frame can be safely applied:

$$\underline{\omega}_b = \begin{Bmatrix} \omega_x \\ \omega_y \\ \omega_z \end{Bmatrix} = \begin{Bmatrix} \dot{\alpha}_x \\ \dot{\alpha}_y \\ \dot{\alpha}_z \end{Bmatrix} + \begin{bmatrix} 1 & \alpha_z & -\alpha_y \\ -\alpha_z & 1 & \alpha_x \\ \alpha_y & -\alpha_x & 1 \end{bmatrix} \begin{Bmatrix} 0 \\ 0 \\ n \end{Bmatrix} \tag{36}$$

It was then examined the difference of the vector ω between the real one and the one computed from the state observer:

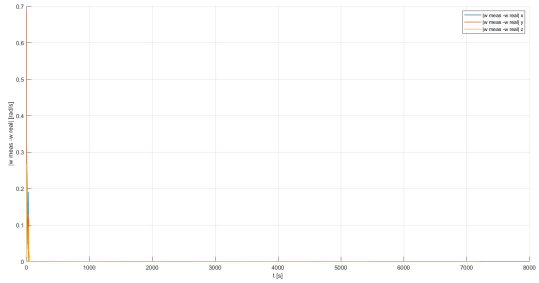

Figure 21: $|\underline{w}_{state\ observer} - \underline{w}_{real}|$

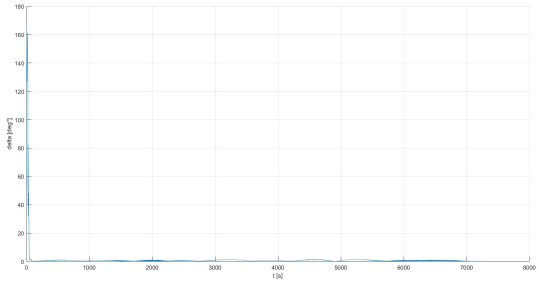

Figure 22: δ

It's possible to notice the initial error of the state observer due to its initial condition $\underline{\omega}_{state\ observer} = [0\ 0\ 0]^T$.

7.2 Control logic

To realise Nadir pointing, the Cubesat has to follow a certain mission profile, with a specific order and logic:

- De-tumbling: spacecraft slow down, using B-dot feedback control,by operating 3 magnetic coils
- Slew manoeuvre: spacecraft points the designed target (Nadir), with a further slow down, using a non-linear Lyapunov control, by operating 3 magnetic coils, 1 Inertia wheel, 1 Reaction wheel
- Nadir Pointing maintenance : spacecraft keeps pointing the designed target, using a non-linear Lyapunov control, by operating 3 magnetic coils, 1 Inertia wheel, 1 Reaction wheel

The conditions to pass from one manoeuvre to the successive was the following:

- De-tumbling → Slew manoeuvre:

$$||\underline{w}_{\text{comp}}|| \leq 2 \times 10^{-2}\,\text{rad/s}$$

[4]

- Slew manoeuvre → Nadir Pointing

$$\begin{cases} ||\underline{w}_{\text{comp}}|| \leq 8.85 \times 10^{-4}\,\text{rad/s} \\ |\alpha_x| + |\alpha_y| + |\alpha_z| \leq 1 \times 10^{-3} \end{cases}$$

8 Actuators

A Reaction Wheel, an Inertial Wheel and 3 Magnetic coils have been implemented as actuators. In this project the actuators receive a specific input signal from the control and generates the effective torque that acts on the satellite, despite the effective torque is different from the control torque due to errors that normally affects actuators.

[4] comp-¿ computed by state observer

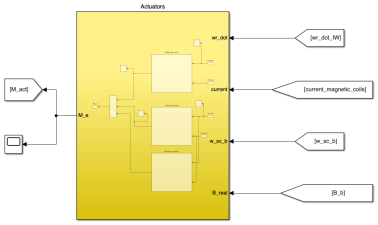

Figure 23: ACTUATORS

8.1 Magnetic coil

Max Voltage	Minimum Magnetic Moment @5V	Magnetic Gain	Linearity [0 − 5V]	Mass	Dimensions [WxHxL]
5 V	1.20 Am^2	8.6 Am^2/A	2.50 %	45 g	13x13x122 mm

Table 6: Cube Torquer Cr0012

The Cubesat is equipped with 3 equal magnetic coils which generate a torque by inducing a magnetic dipole in a coil, interacting with the Earth's magnetic field, generating a torque.

$$\underline{M} = \underline{D} \times \underline{B} \tag{37}$$

where: $\underline{D} = \mu\, N\, S\, \underline{i}$ is the magnetic dipole, where the current is the control variable.
The torque depends directly from the external environment, generating a variable torque not only due to the dipole; furthermore they have to be placed far from the Cubesat's main core, in order to avoid undesired disturbances caused by electromagnetic interference from wires and electronics. It is never possible to generate three independent components of the control torque, as we can change $\underline{M}$ only on a plane orthogonal to $\underline{B}$:

$$\underline{D} = [-B\wedge]^{-}1\, \underline{M} \tag{38}$$

The solution to this problem is shown in Chapter 8.2.
The 3 magnetic coils are mounted along the 3 axis of the body frame, therefore the DCM of the actuators axis respect to the body frame is:

$$A_{magn\, act/b} = \begin{bmatrix} 1 & 0 & 0 \\ 0 & 1 & 0 \\ 0 & 0 & 1 \end{bmatrix} \tag{39}$$

This rotation matrix is , in general, useful to compute the input current for each magnetic coil, as eq.38 is written in body frame. During the computation from input current to the effective torque produced, it has been taken into account an orthogonality error of the actuators, due to their not precise mounting on the satellite. This procedure is therefore shown:

$$\underline{D}_{act} = (I_3 - [ortho_{error}\wedge])\mu\, N\, S\, \underline{i}_{control} \tag{40}$$ [5]

8.2 Reaction and Inertia Wheels

	Size (HxR) [mm]	Mass [g]	Max Speed [RPM]	Random vibration [gRMS]	Saturation Torque [mNm]	Nominal Motor Supply Voltage [V]
RW	11x15	400	10000	14.16	10	12
IW	13.75x19	600	10000	14.16	15	16

Table 7: RW CubeWheel CW0500 / IW CubeWheel CW1200

[5] N: number of coils windings

By using Magnetic coils it is not possible to generate three independent components of the control torque, therefore at least another actuator is necessary, such as a Reaction Wheel (RW) and/or an Inertia Wheel (IW). Therefore the control can be modeled as:

$$\underline{M} = \begin{bmatrix} -B\wedge & A_{b/W} \end{bmatrix} \begin{Bmatrix} \underline{D} \\ \dot{\underline{h}}_r \end{Bmatrix} \tag{41}$$

The input of the actuators is computed as follows:

$$\begin{Bmatrix} \underline{D} \\ \dot{\underline{h}}_r \end{Bmatrix} = \begin{bmatrix} -B\wedge & A_{b/W} \end{bmatrix}^{+} \underline{M} \tag{42}$$

[6]

where $\dot{\underline{h}}_r = I_r \dot{\underline{\omega}}_r$ is the rate of change of angular momentum of the Wheel. Matrix $A_{\mathrm{b/W}}$ is composed by three rows and as many columns as number of Wheels. Each column represents the direction of the axis of rotation of the Wheel. As explained in Chapter 4.2, the IW is necessary in order to guarantee a dual spin stabilization of the spacecraft which rotates around the minimum inertia axis. IW's spin axis orientation[7] with respect to the body frame is therefore expressed by:

$$A_{b/IW} = [0\ 0\ 1]' \tag{43}$$

Indeed, the RW may have an arbitrary orientation. In order to always guarantee the control of the s/c, the wheel's spin axis has to be aligned with a non-zero local value of the magnetic field at each time step, in such a way that the wheel is capable to generate the missing torque.
An accurate study of the magnetic field model in body frame has been performed in the specific case of the Sun-synchronous orbit considered in order to understand if the IW at issue satisfies the condition of non-zero B or if a RW need to be implemented too.
Figure 24 shows the projection of the magnetic field in body frame along the RW spin axis as its orientation changes, whereas Figure 25 shows the projection of the magnetic field in body frame along the IW (both during one orbital period).

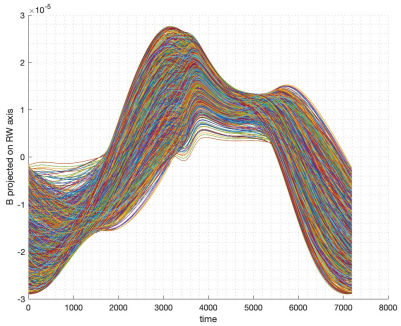

Figure 24: B projection on RW spin axis

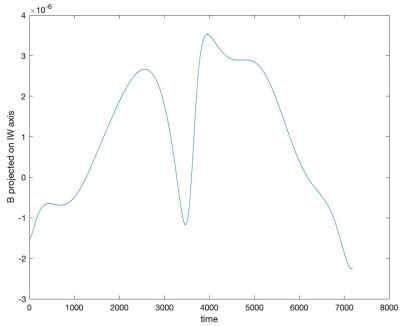

Figure 25: B projection on IW spin axis

The reason why an IW is not enough, can be deduced from Figure 25: the projection of B_b along its spin axis passes through zero four times per period. A possible solution is to use both a RW and an IW. Although the projection of B_b along the RW's spin axis passes through zero twice a period (Figure 24) for any orientation, it is possible to find a configuration that guarantees that the wheels work alternately, always generating the missing torque. Moreover, the criterion to determine the optimal RW's axis orientation, is to choose the one along which the magnetic field

[6] + denotes the pseudoinverse of the matrix
[7] IW is aligned with minimum inertia axis of satellite

has the maximum absolute mean value. For our specific case, the optimal RW axis orientation with respect to body frame has been found to be:

$$A_{b/RW}^{opt} = [0.9948\ 0.0697\ 0.0748]^T \tag{44}$$

In Simulink model, the value of Saturation Torque has been taken into account when evaluating the Control Torque M_c. Moreover, it has been verified that the angular velocity of the wheels does not exceed the maximum speed value reported in the data sheet (see Figure 27).

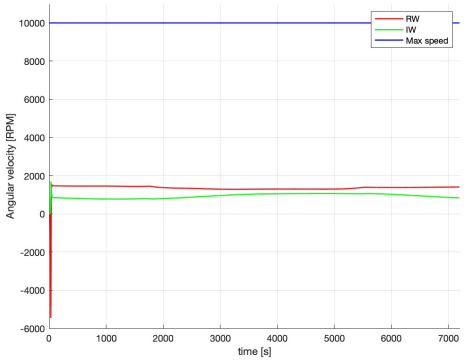

Figure 26: RW and IW angular velocity ω_B

Therefore, no problems due to saturation have been found.
For completeness, it have been analyzed the case with three magnetic coils and one reaction wheel (RW) for spacecraft control has drawbacks. These include instability in the minor axis, necessitating a change in the spacecraft body frame for rotation around its major inertia axis. There is also an issue with the singularity of the pseudoinverse matrix in Eq42.
Moreover, typical Earth sensing missions require pointing the spacecraft's major surface towards the Earth to maximize measurements and facilitate communication with ground stations. Unfortunately, this orientation hinders the possibility of spinning around the spacecraft's major axis.
To address both issues, a configuration with both RW and inertial wheels (IW) is necessary.

9 Pointing results

The Cubesat's initial condition is characterized with a random attitude and angular velocity,depending only on the launcher and satellite deployment :

- $\underline{w}_{0\ b} = [-0.1745\ 0.1623\ 0.1396]^T\ rad/s$
- $[\underline{\phi}\ \theta\ \psi]_0^{T\ [8]} = [1.6394\ \ -0.5245\ \ -0.6304]^T\ rad$

Following the control strategy showed in Chapter 7.2, the performance of the mission during the various phases in terms of real angular velocity and real attitude error are reported.

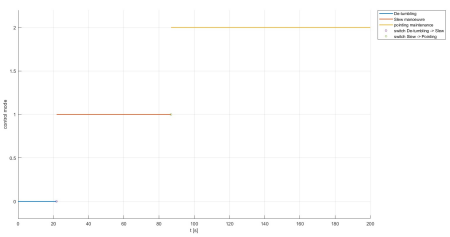

Figure 27: switch between the mission phases, with zoom for the first $200s$

[8] 312 configuration

- De-tumbling with 3 magnetic coils: it takes 21.8 s to slow down the Cubesat, without paying attention to the spacecraft attitude.

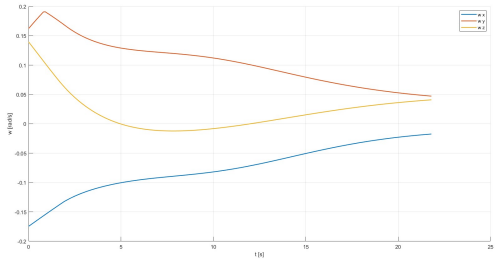

Figure 28: $\underline{w}_{detumbling}$

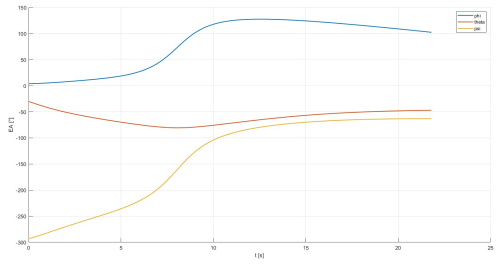

Figure 29: Euler Angles attitude error

Figure 30: performance De-tumbling

- Slew manoeuvre with 3 magnetic coils, 1 Inertia Wheel, 1 Reaction Wheel: from the former state the Cubesat starts to accelerate the inertia and reaction wheel, achieving the correct pointing, slowing further down the spacecraft in $65,0$ s. The peaks of $\underline{w}$ are due to the forced rotation to achieve the correct pointing in a short time.

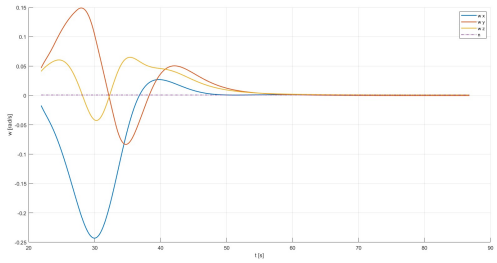

Figure 31: $\underline{w}_{slew}$

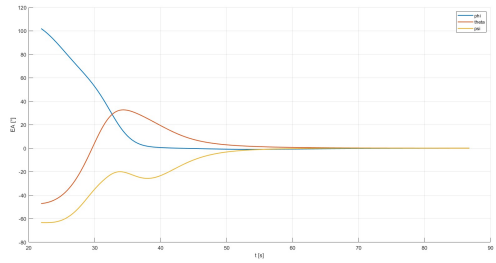

Figure 32: Euler Angles attitude error

Figure 33: performance Slew

- Nadir Pointing maintenance with 3 magnetic coils, 1 Inertia Wheel, 1 Reaction Wheel: the Cubesat realises micro-corrections in order to maintain the correct pointing.The oscillations of $\underline{w}$ and attitude error are linked to small errors carried by instruments (sensors, actuators), on-board computer, which works in a time-discrete domain , the environmental disturbances; the control logic necessarily needs a certain interval to correct properly the performances. The maximum attitude error is under 2 deg, as expected with the equipped attitude control architecture on the Cubesat 12U.

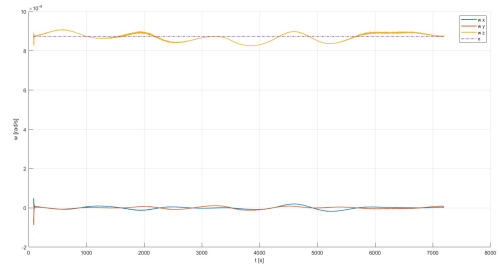

Figure 34: $\underline{w}_{point}$

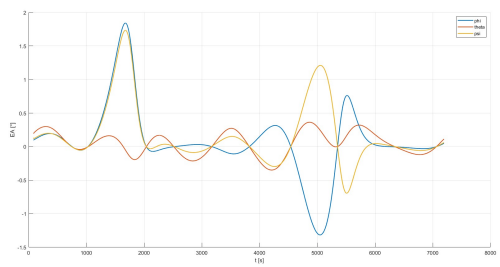

Figure 35: Euler Angles attitude error

Figure 36: performance Nadir Pointing

They are reported the total performances:

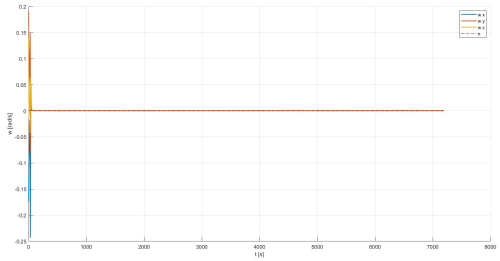

Figure 37: $\underline{w}$

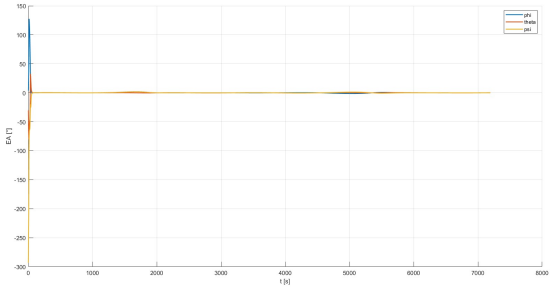

Figure 38: Euler Angles attitude error

Figure 39: complete mission performance

10 Conclusion

In this report a 12U Cubesat attitude control simulation over a Sun-synchronous orbit is presented. The target chosen is Nadir pointing. The academic purpose and project's requirements make the model a simplified version of a real design. Indeed, no redundancies have been taken into account, trying to use the minimum set of sensors and actuators that in normal condition (i.e., no emergency situations, no brake of components) allow the spacecraft to properly achieve its mission during its whole life.

An important observation about the choice of a Sun-synchronous orbit should be done. First of all, the project specifications required the implementation of Sun-sensors, Magnetic coils as well as an Inertia Wheel. In order to use Magnetic coils, a Magnetometer is necessary, because an evaluation of the local magnetic field is required to compute the control action. Therefore, two good possibilities in terms of orbit to be performed were possible, both with advantages and drawbacks:

- Equatorial Orbit
  - Disadvantage: another sensor - such as an Horizon Sensor - need to be added because solar eclipses have to be considered.
  - Advantage: no more actuators to be added. In fact, the pitch axis (along which the IW is oriented) is the direction along which the magnetic field is not only non-zero but also maximum.
- Sun-synchronous Orbit
  - Disadvantage: as explained in Chapter 8 another actuator is required if we want the s/c to be controlled at each time step.
  - Advantage: no more sensors required because (see Chapter 6.1).

In this project the second choice has been developed, and a Reaction Wheel has been implemented in addition to the Inertia Wheel.

11 Bibliography

- CubeSpace, Gen 2 ADCS Actuators link
- AAC Clyde Space, MAG-3 Satellite Magnetometer link
- AAC Clyde Space,SS200 Sun Sensor link
- David A. Vallado, Fundamentals of Astrodynamics and Applications,Microcosm Press.
- Cubesat 12U link
- Bernelli Franco Zazzera, Spacecraft Attitude Dynamics notes, AY 2023/2024